Gut Microbiomes of Malawian Twin Pairs Discordant for Kwashiorkor

Michelle I. Smith *et al.*

Science **339**, 548 (2013);
DOI: 10.1126/science.1229000

Science (print ISSN 0036-8075; online ISSN 1095-9203) is published weekly, except the last week in December, by the American Association for the Advancement of Science, 1200 New York Avenue NW, Washington, DC 20005.

potential, especially during stress. The contribution of diversity-generating mechanisms such as epigenetic regulation, noise in gene expression, or variability in the microenvironment (*21*, *22*) may offer insight into CRC cell heterogeneity.

There is growing evidence of evolutionary selection for diversity-generating mechanisms in other disciplines, such as ecology (*23*, *24*) and microbiology (*25*–*27*). For example, genetically homogeneous pools of single-cell prokaryotes display heterogeneity, where a small portion of cells naturally display drug resistance that is not caused by genetic mutation or acquisition of plasmids encoding antibiotic resistance genes. Rather, this phenomenon is due to mechanisms that reduce cell proliferation and induce a dormant nondividing state (*28*). We consistently observed a relatively dormant cell population in CRC, which suggests that cancer cells may take advantage of this "ancient" mechanism and use dormancy as an adaptive strategy during times of stress. We provide evidence for a relatively dormant or slowly proliferating cell population in primary human CRC cells that still retains potent tumor propagation potential, thereby preferentially driving tumor growth after chemotherapy. These findings may provide a biological basis for recurrent and metastatic disease following standard-of-care treatment (*29*). Our findings should focus efforts to uncover the molecular mechanisms driving chemotherapeutic tolerance in CRC cells.

The often unstated assumption in considering cellular response to stress is that cells react in a uniform manner to the inducing signal, because the classical techniques used bulk populations. However, averaging data across millions of cells has the effect of masking any heterogeneity that might exist at the single-cell level. Such conventions are changing as methodological advances (*30*) are fueling a surge of interest in the processes governing cell-to-cell variability (*14*). By coupling genetic analysis to functional tumor growth assays, we find that when cells are tracked at single-cell resolution while still being part of a population of cancer cells, variable cellular behaviors can be detected. These observations set a precedent for future studies examining the basis of intraclonal behavior of single cells, especially with respect to tumor propagation and other functional properties. In a broader sense, our findings reveal another layer of complexity, beyond genetic diversity, that drives the intratumoral heterogeneity of CRC. The prospect of understanding how genetic and nongenetic determinants interact to influence the functional diversity and therapy response for other cancers should drive future cancer research.

References and Notes

1. M. Greaves, C. C. Maley, *Nature* **481**, 306 (2012).
2. S. Nik-Zainal *et al.*; Breast Cancer Working Group of the International Cancer Genome Consortium, *Cell* **149**, 994 (2012).
3. M. Gerlinger *et al.*, *N. Engl. J. Med.* **366**, 883 (2012).
4. K. Anderson *et al.*, *Nature* **469**, 356 (2011).
5. F. Notta *et al.*, *Nature* **469**, 362 (2011).
6. E. Clappier *et al.*, *J. Exp. Med.* **208**, 653 (2011).
7. C. G. Mullighan *et al.*, *Science* **322**, 1377 (2008).
8. X. Wu *et al.*, *Nature* **482**, 529 (2012).
9. W. Liu *et al.*, *Nat. Med.* **15**, 559 (2009).
10. M. E. Gorre *et al.*, *Science* **293**, 876 (2001).
11. C. Roche-Lestienne, J. L. Laï, S. Darré, T. Facon, C. Preudhomme, *N. Engl. J. Med.* **348**, 2265 (2003).
12. M. J. Bissell, M. A. Labarge, *Cancer Cell* **7**, 17 (2005).
13. V. Sanz-Moreno *et al.*, *Cell* **135**, 510 (2008).
14. S. L. Spencer, S. Gaudet, J. G. Albeck, J. M. Burke, P. K. Sorger, *Nature* **459**, 428 (2009).
15. A. Roesch *et al.*, *Cell* **141**, 583 (2010).
16. S. V. Sharma *et al.*, *Cell* **141**, 69 (2010).
17. P. B. Gupta *et al.*, *Cell* **146**, 633 (2011).
18. K. Ishizawa *et al.*, *Cell Stem Cell* **7**, 279 (2010).
19. P. N. Kelly, A. Dakic, J. M. Adams, S. L. Nutt, A. Strasser, *Science* **317**, 337 (2007).
20. S. Jones *et al.*, *Proc. Natl. Acad. Sci. U.S.A.* **105**, 4283 (2008).
21. A. Marusyk, V. Almendro, K. Polyak, *Nat. Rev. Cancer* **12**, 323 (2012).
22. M. Kærn, T. C. Elston, W. J. Blake, J. J. Collins, *Nat. Rev. Genet.* **6**, 451 (2005).
23. M. Loreau *et al.*, *Science* **294**, 804 (2001).
24. D. F. Flynn, N. Mirotchnick, M. Jain, M. I. Palmer, S. Naeem, *Ecology* **92**, 1573 (2011).
25. H. B. Fraser, A. E. Hirsh, G. Giaever, J. Kumm, M. B. Eisen, *PLoS Biol.* **2**, e137 (2004).
26. H. L. True, S. L. Lindquist, *Nature* **407**, 477 (2000).
27. J. M. Raser, E. K. O'Shea, *Science* **304**, 1811 (2004).
28. K. Lewis, *Nat. Rev. Microbiol.* **5**, 48 (2007).
29. A. M. Abulafi, N. S. Williams, *Br. J. Surg.* **81**, 7 (1994).
30. J. M. Raser, E. K. O'Shea, *Science* **309**, 2010 (2005).

Acknowledgments: We thank L. Gibson, A. Khandani, and P. Penttila for experimental support and members of the Dick lab, especially M. Doedens, J. Wang, M. Milyavsky, and E. Laurenti for technical support and critical assessment of this work, as well as UHN biobank for specimens, the Clinical Applications of Core Technology (Affymetrix) Laboratory of the Hartwell Center for Bioinformatics and Biotechnology of St. Jude Children's Research Hospital, and the American Lebanese Syrian Associated Charities of St. Jude Children's Research Hospital. Supported by Genome Canada through the Ontario Genomics Institute, Ontario Institute for Cancer Research and a Summit Award with funds from the province of Ontario, the Canadian Institutes for Health Research, the Netherlands Organisation for Scientific Research, NIH grant R21 CA149990-01, a Canada Research Chair, the Princess Margaret Hospital Foundation, and the Ontario Ministry of Health and Long Term Care (OMOHLTC). The views expressed do not necessarily reflect those of the OMOHLTC.

Supplementary Materials

www.sciencemag.org/cgi/content/full/science.1227670/DC1
Materials and Methods
Supplementary Text
Figs. S1 to S17
Tables S1 to S13
References (*31*–*56*)

19 July 2012; accepted 26 November 2012
Published online 13 December 2012;
10.1126/science.1227670

Gut Microbiomes of Malawian Twin Pairs Discordant for Kwashiorkor

Michelle I. Smith,[1]* Tanya Yatsunenko,[1]* Mark J. Manary,[2,3,4] Indi Trehan,[2,3] Rajhab Mkakosya,[5] Jiye Cheng,[1] Andrew L. Kau,[1] Stephen S. Rich,[6] Patrick Concannon,[6] Josyf C. Mychaleckyj,[6] Jie Liu,[7] Eric Houpt,[7] Jia V. Li,[8] Elaine Holmes,[8] Jeremy Nicholson,[8] Dan Knights,[9,10]† Luke K. Ursell,[11] Rob Knight,[9,10,11,12] Jeffrey I. Gordon[1]‡

Kwashiorkor, an enigmatic form of severe acute malnutrition, is the consequence of inadequate nutrient intake plus additional environmental insults. To investigate the role of the gut microbiome, we studied 317 Malawian twin pairs during the first 3 years of life. During this time, half of the twin pairs remained well nourished, whereas 43% became discordant, and 7% manifested concordance for acute malnutrition. Both children in twin pairs discordant for kwashiorkor were treated with a peanut-based, ready-to-use therapeutic food (RUTF). Time-series metagenomic studies revealed that RUTF produced a transient maturation of metabolic functions in kwashiorkor gut microbiomes that regressed when administration of RUTF was stopped. Previously frozen fecal communities from several discordant pairs were each transplanted into gnotobiotic mice. The combination of Malawian diet and kwashiorkor microbiome produced marked weight loss in recipient mice, accompanied by perturbations in amino acid, carbohydrate, and intermediary metabolism that were only transiently ameliorated with RUTF. These findings implicate the gut microbiome as a causal factor in kwashiorkor.

Malnutrition is the leading cause of child mortality worldwide (*1*). Moderate acute malnutrition (MAM) refers to simple wasting with a weight-for-height *z* (WHZ) score between two and three standard deviations below the median defined by World Health Organization (WHO) Child Growth Standards (*2*, *3*). Severe acute malnutrition (SAM) refers to either marasmus, which is extreme wasting with WHZ scores less than –3, or kwashiorkor, a virulent form of SAM characterized by generalized edema, hepatic steatosis, skin rashes and ulcerations, and anorexia (*4*, *5*). The cause of kwashiorkor remains obscure. Speculation regarding its pathogenesis has focused on inadequate protein intake and/or excessive oxidative stress, but substantial evidence to refute these hypotheses has come from epidemiologic surveys and clinical trials (*6*–*9*). Our comparative metagenomic study of the gut microbiomes of 531 healthy infants, children, and adults living in the United States, Venezuela, and Malawi revealed a maturational program in which the proportional representation of genes encoding functions related to micro- and macronutrient biosynthesis and metabolism changes during postnatal development (*10*). Together, these observations give rise to the following testable hypotheses: (i) The gut microbiome provides essential functions needed for healthy postnatal growth and development; (ii) disturbances in microbiome assembly and function (for instance, those prompted by

enteropathogen infection) affect the risk for kwashiorkor; and (iii) in a self-reinforcing pathogenic cascade, malnutrition affects the gut microbiome functions involved in determining nutritional status, thus further worsening health status. To complicate matters, several gut microbiome configurations may be associated with kwashiorkor among different hosts and even within a given host over time. Moreover, microbiome configurations associated with kwashiorkor may be differentially affected by therapeutic food interventions, and features that are reconfigured during treatment may not persist after withdrawal of treatment.

To address some of these hypotheses, we performed a longitudinal comparative study of the fecal microbiomes of monozygotic (MZ) and dizygotic (DZ) twin pairs born in Malawi who became discordant for kwashiorkor. Malawi has one of the highest infant mortality rates in the world (*1*, *11*). We reasoned that a healthy (well-nourished) co-twin in a discordant twin pair represented a very desirable control, given his or her genetic relatedness to the affected co-twin and the twins' similar exposures to diet and microbial reservoirs in their shared early environment. Ready-to-use therapeutic food (RUTF) composed of peanut paste, sugar, vegetable oil, and milk fortified with vitamins and minerals has become the international standard of treatment for SAM in community-based treatment programs (*12*). In Malawi, the standard of care for twins discordant for kwashiorkor is to treat both co-twins with RUTF to limit food sharing; this practice allowed us to compare and contrast their microbiomes before, during, and after treatment. Following each child in a twin pair prospectively permitted each individual to serve as his or her own control. Moreover, if there are many different routes to disrupted microbiome structure and/or function, then each discordant twin pair could provide an illustration of underlying pathology. As an additional set of controls, we defined temporal variation of the fecal microbiomes in twin pairs who remained well nourished, lived in the same geographic locations as discordant pairs, and never received RUTF.

Regardless of their health status, a total of 317 twin pairs younger than 3 years old, from five villages in the southern region of Malawi, were enrolled in our study. We followed these children until they reached 36 months of age. Zygosity testing (*13*) revealed that 46 (15%) twin pairs were MZ. We used WHO criteria (*3*) to diagnose kwashiorkor based on the presence of bilateral pitting pedal edema, marasmus when a child had a WHZ score less than –3, and MAM when the WHZ score was between –2 and –3 and bilateral pitting pedal edema was absent (*2*, *3*). We treated SAM with RUTF and MAM with a soy-peanut ready-to-use supplementary food (*14*). After diagnosis with SAM, we assessed anthropometry and collected a fecal sample every 2 weeks until the child recovered (defined as WHZ score greater than –2 and no edema).

Fifty percent of twin pairs remained well nourished throughout the study, whereas 43% became discordant, and 7% manifested concordance for acute malnutrition. The prevalence of discordant compared with concordant phenotypes was significantly different ($P < 10^{-15}$, binomial and χ^2 tests). MAM was significantly more frequent than SAM, affecting 81 (60%) of the 135 discordant twin pairs ($P = 0.02$, χ^2 test) (table S1A). Of the 634 children in the study, 7.4% developed kwashiorkor, 2.5% had marasmus, and 13.9% were diagnosed with MAM; 10.7% had multiple episodes of malnutrition, with the most frequent combination being marasmus and MAM (5.5% of the children) (table S1B). There was no significant relationship between concordance for acute malnutrition and zygosity, nor did we find significant differences in the number of MZ versus DZ twin pairs affected with kwashiorkor, marasmus, or MAM in our cohort ($\chi^2$and Fisher's exact tests). Taking all 135 discordant pairs into account, there was no statistically significant difference in the incidence of discordance for kwashiorkor, marasmus, or MAM in MZ versus DZ twin pairs (table S1A). In addition, we did not find any association between gender or geographic location and the type or incidence of malnutrition or in the discordance rate for MAM or SAM among twin pairs (table S1, B and C). For the current study, we chose to focus on children with kwashiorkor because: (i) survival of both members of a twin pair with kwashiorkor was significantly higher than with marasmus; (ii) onset occurred at a later age, allowing us to better assess the state of functional development of the gut microbiome; (iii) the duration of RUTF treatment was more uniform than in cases of marasmus; and (iv) there was a lower incidence of relapse to SAM (see supplementary text for additional details).

Microbiomes of healthy twins and pairs discordant for kwashiorkor. We selected nine same-gender twin pairs who remained well nourished in our study cohort and 13 of 19 same-gender twin pairs who became discordant for kwashiorkor for metagenomic analyses of their microbiomes [n = 5 MZ and 4 DZ healthy pairs and 7 MZ and 6 DZ pairs discordant for kwashiorkor; for 12 of the 13 discordant pairs, there was a single episode of kwashiorkor during the study period] (see supplementary text for the criteria used for participant selection and table S2A for additional information about participants and their samples). DNA prepared from fecal samples was subjected to multiplex shotgun pyrosequencing, and the resulting reads were annotated by comparison to the Kyoto Encyclopedia of Genes and Genomes (KEGG) database and to a database of 462 sequenced human gut microbes (table S3). To visualize the variation in this data set, we used principal coordinates analysis of Hellinger distances computed from the KEGG enzyme commission number (EC) content of fecal microbiomes (Fig. 1A and fig. S1). Principal coordinate 1 (PC1), which explained the largest amount of variation, was strongly associated with age and family membership (Fig. 1A). Because age encompasses a variety of metabolic and dietary changes, we used the positions of microbiomes along PC1 to assess functional development of the microbiomes of twin pairs who remained healthy and twin pairs who became discordant for kwashiorkor. When microbiomes from three consecutive time points from twins who remained healthy were plotted along PC1, there was a steady progression toward a configuration found in older children (Fig. 1B). We observed a similar result in healthy co-twins from discordant twin pairs. This was not the case for their siblings with kwashiorkor: Their fecal microbiomes, sampled at the time of diagnosis, as well as during and following administration of RUTF, did not show significant differences in their positions in the ordination plot (Fig. 1C). We obtained the same results for KEGG orthology groups. We used Fisher's exact test to compare the representation of KEGG ECs between a healthy and a malnourished co-twin within each family, and we identified ECs that were significantly different in as few as one and as many as six of the twin pairs (table S5).

These associations between the configurations of gut microbial communities and health status do not establish whether the microbiome is a causal factor in the pathogenesis of kwashiorkor. We reasoned that transplanting previously frozen fecal microbial communities, obtained from discordant twin pairs at the time one of the co-twins presented with kwashiorkor, into gnotobiotic mice would allow us to assess the degree to which donor phenotypes could be transmitted via their gut microbiomes and to identify features of microbial community structure, metabolism, and host-microbial cometabolism associated with donor health status and diet. In the absence of a distinct and consistent taxonomic signature of kwashiorkor (supplementary text), we selected pretreatment fecal samples from three discordant twins based on the following criteria: All twin pairs were of similar age, and neither co-twin in any pair had diarrhea or vomiting or was consuming antibiotics at the time that fecal samples were collected.

[1]Center for Genome Sciences and Systems Biology, Washington University in St. Louis, St. Louis, MO 63110, USA. [2]Department of Pediatrics, Washington University in St. Louis, St. Louis, MO 63110, USA. [3]Department of Community Health and Department of Pediatrics and Child Health, University of Malawi College of Medicine, Blantyre, Malawi. [4]U.S. Department of Agriculture Children's Nutrition Research Center, Baylor College of Medicine, Houston, TX 77030, USA. [5]Department of Microbiology, College of Medicine, University of Malawi, P/B 360, Chichiri, Blantyre 3, Malawi. [6]Center for Public Health Genomics, University of Virginia, Charlottesville, VA 22904, USA. [7]Division of Infectious Diseases and International Health, University of Virginia, Charlottesville, VA 22908, USA. [8]Biomolecular Medicine, Department of Surgery and Cancer, Faculty of Medicine, Imperial College London, London SW7 2AZ, UK. [9]Department of Computer Science, University of Colorado, Boulder, CO 80309, USA. [10]Biofrontiers Institute, University of Colorado, Boulder, CO 80309, USA. [11]Department of Chemistry and Biochemistry, University of Colorado, Boulder, CO 80309, USA. [12]Howard Hughes Medical Institute, University of Colorado, Boulder, CO 80309, USA.

*These authors contributed equally to this work.

†Present address: Department of Computer Science and Engineering and BioTechnology Institute, University of Minnesota, Saint Paul, MN 55108, USA.

‡To whom correspondence should be addressed. E-mail: jgordon@wustl.edu

The twins selected included DZ pair 196 (aged 16.5 months), DZ pair 56 (aged 18 months), and MZ twin pair 57 (aged 21 months) (see fig. S5 and table S2A for clinical characteristics).

Transplantation of fecal microbial communities into gnotobiotic mice. Fecal microbiota samples from the six selected human donors were each transplanted, with a single oral gavage, into separate groups of adult 8-week-old male C57BL/6J germ-free mice. Beginning 1 week before gavage, animals were freely fed a sterilized diet based on the staple foods consumed by individuals living in rural southern Malawi (see table S6 for the composition of this low caloric density, nutrient-deficient diet and fig. S6 for experimental design) (*10*). In two of the three discordant twin pairs (families 196 and 57), transplantation of the kwashiorkor co-twin's microbiota resulted in significantly greater weight loss in recipient mice over the ensuing 3 weeks than in those harboring the healthy sibling's microbiota (Fig. 2A). This discordant weight loss phenotype was dependent on the combination of Malawian diet and kwashiorkor microbiota; when separate groups of animals were placed on a standard mouse chow, there were no significant differences between the weights of mice with kwashiorkor compared to healthy co-twin microbiota (93.6 ± 4% versus 93 ± 11% of their starting weights after 21 days, respectively) or compared to mice with a healthy co-twin microbiota consuming a Malawian diet (102.4 ± 11.1%).

Three weeks after gavage, mice consuming the Malawian diet were switched to the RUTF given to children with SAM. At the time of the diet switch, all recipients of kwashiorkor microbiota from families 196 and 57 had become severely anorectic. All mice in each treatment group rapidly gained weight while consuming RUTF. In the case of the most discordant set of recipients (from family 196), mice with the kwashiorkor co-twin's microbiota did not achieve the same body weight as recipients of the healthy sibling's microbiota, but these mice did reach 96.8 ± 2.8% of their pre-gavage weight. After 2 weeks on RUTF, all mice in all treatment groups were returned to the Malawian diet. Whereas all recipients of microbiota transplants lost weight, this re-exposure did not produce the profound weight loss that mice colonized with the kwashiorkor microbiota had experienced during their first exposure (Fig. 2A). These results indicate that the gut microbiota from two of the three discordant pairs are able to transmit a discordant malnutrition phenotype, manifested by weight loss, to recipient gnotobiotic mice. Given that the most discordant weight loss phenotype was produced by microbiota from twin pair 196, we initiated a detailed time-series analyses of the organismal, gene, and metabolite content of the transplanted microbial communities as a function of co-twin donor and diet (fig. S6 and table S2, B and C).

Transplantation was efficient: (i) 62 of 72 species-level taxa present in the input community from the healthy co-twin and 58 of 67 species-level taxa from the kwashiorkor co-twin were detected in fecal microbiota collected from all transplant recipients across time points and diets (table S7); (ii) 90.6 and 89.6% of the 859 ECs detected in each of the healthy and kwashiorkor input communities were identified in the fecal microbiota of transplant recipients after 3 weeks on the Malawian diet; and (iii) the proportional representation of ECs in input versus output fecal communities was highly correlated (correlation coefficient R^2 = 0.893 to 0.936) (fig. S7, A and B). Polymerase chain reaction–Luminex assays (*15*–*18*) for 22 common bacterial, parasitic, and viral enteropathogens in the input human microbiota, as well as in recipient mouse fecal samples, indicated that the markedly discordant weight loss phenotype in recipients of these microbiota was not due to transfer and/or subsistence of any of the surveyed pathogens (fig. S8, A and B, and supplementary text).

Comparison of the two groups of gnotobiotic recipients while they consumed a Malawian diet showed significant differences in the proportional representation of 37 species-level taxa. Organisms with the most statistically significant differences, and whose relative proportions were higher in mice with the kwashiorkor microbiota, were (i) *Bilophila wadsworthia*, a hydrogen-consuming, sulfite-reducing organism that is related to members of *Desulfovibrio* (phylum Proteobacteria) and has been linked to inflammatory bowel disease (IBD) in humans and induces a proinflammatory T helper 1 response in a mouse model of IBD (*19*), and (ii) *Clostridium innocuum*, a gut symbiont that can function as an opportunist in immunocompromised hosts (table S8B) (*20*). *B. wadsworthia* and members of the order Clostridiales were also overrepresented in the fecal microbiota of the kwashiorkor co-twin from family 196 compared with his healthy co-twin at the time he presented with kwashiorkor (table S8B).

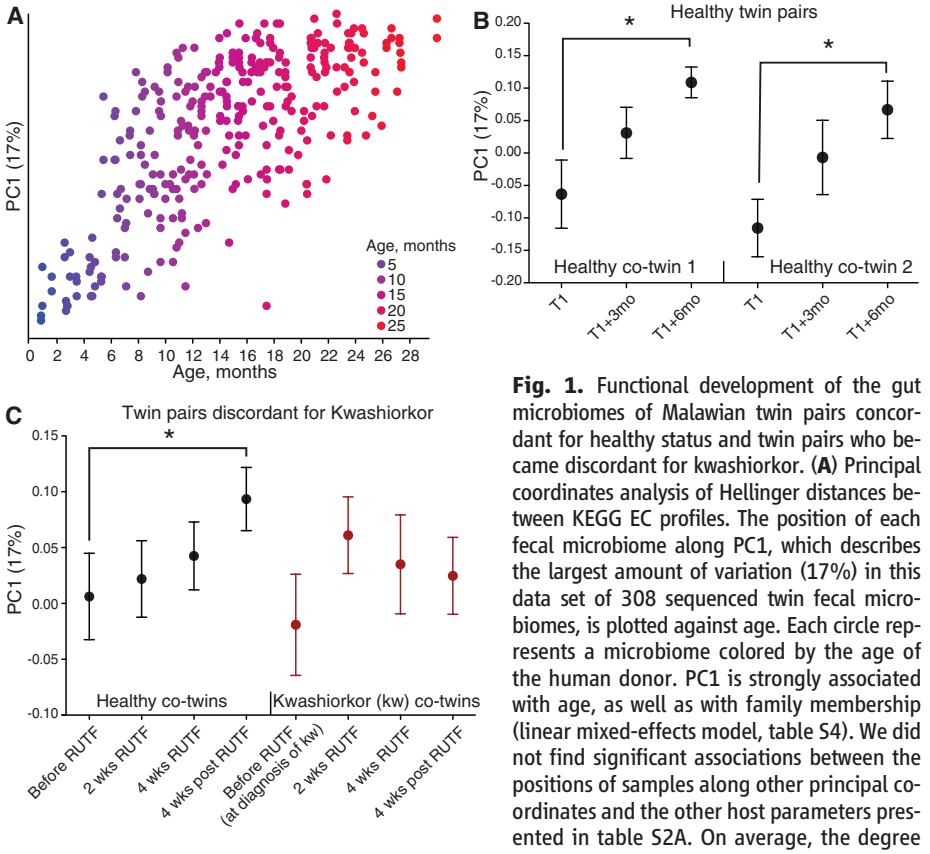

Fig. 1. Functional development of the gut microbiomes of Malawian twin pairs concordant for healthy status and twin pairs who became discordant for kwashiorkor. (**A**) Principal coordinates analysis of Hellinger distances between KEGG EC profiles. The position of each fecal microbiome along PC1, which describes the largest amount of variation (17%) in this data set of 308 sequenced twin fecal microbiomes, is plotted against age. Each circle represents a microbiome colored by the age of the human donor. PC1 is strongly associated with age, as well as with family membership (linear mixed-effects model, table S4). We did not find significant associations between the positions of samples along other principal coordinates and the other host parameters presented in table S2A. On average, the degree of intrapersonal variation in a co-twin was not smaller than the variation between co-twins (fig. S2). Similar to twins who remained healthy, the temporal variation within a co-twin member of a discordant twin pair was equal to the variation between co-twins, but still smaller compared with unrelated children (fig. S2). (**B**) Average ± SEM (error bars) PC1 coordinate obtained from the data shown in (A) for microbiomes sampled at three consecutive time points from nine twin pairs who remained well nourished (healthy) during the study (participants surveyed between 3 weeks and 24.5 months of age). (**C**) Average ± SEM (error bars) PC1 coordinate obtained from (A) for microbiomes sampled before, during, and after RUTF treatment from co-twins discordant for kwashiorkor. *P < 0.05, Friedman test with Dunn's post-hoc test applied to data shown in (B) and (C). Similar results were obtained using other distance metrics [Bray Curtis, Euclidian, and Kulzyncki (fig. S3)]. (See also fig. S4, which shows how changes in the relative proportion of Actinobacteria parallel the patterns observed with the changes along PC1. Children with kwashiorkor manifested a statistically significant decrease in Actinobacteria with the introduction of RUTF, unlike their healthy co-twins).

Switching from a Malawian diet to RUTF produced a rapid change in configuration of the fecal microbiota that was most pronounced in recipients of the kwashiorkor co-twin's community (Fig. 2B and fig. S9, A and B). Thirty species-level taxa exhibited statistically significant changes in their representation in kwashiorkor microbiota transplant recipients (Fig. 2C and tables S7B and S8A), with prominent increases in *Bifidobacteria* (*B. longum*, *B. bifidum*, plus another unclassified taxon), two *Lactobacilli* [*L. reuteri* and *L. gasseri*, which can produce bacteriocins and stimulate the innate immune system to inhibit the growth and eliminate various enteropathogens (*21*–*23*)], and two members of *Ruminococcus* [*R. torques*, a mucus degrader (*24*), and *Faecalibacterium prausnitzii*, a member of the order Clostridiales that exhibits anti-inflammatory activity in a mouse model of colitis and whose decreased representation is associated with increased risk of ileal Crohn's disease (*25*)]. We observed statistically significant decreases in the representation of members of the Bacteroidales (*B. uniformis*, *Parabacteroides distasonis*, plus an unclassified *Parabacteroides* taxon) (see Fig. 2C and legend for time courses). Twenty-eight bacterial species-level taxa also exhibited significant changes in their representation in gnotobiotic mice harboring the healthy co-twin's microbiota in response to RUTF. The pattern of change of 13 different taxa—including the two *Ruminococcus* spp., *B. uniformis*, *P. distasonis*, *B. longum*, and an unclassified *Bifidobacterium* taxon—was shared by both recipient groups (healthy and kwashiorkor), although the *Bifidobacterium* response was less pronounced in the healthy microbiota

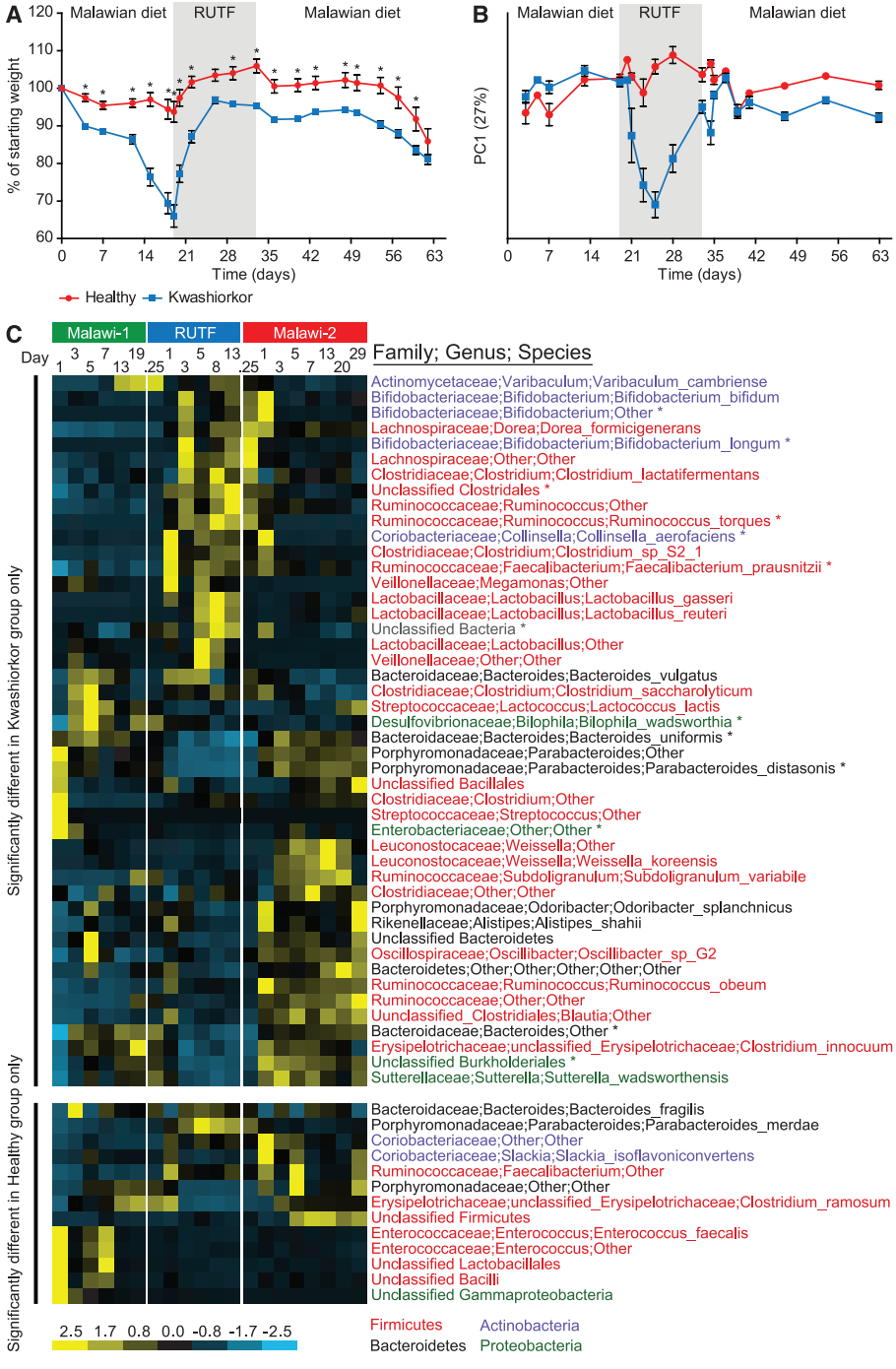

Fig. 2. Transplantation of fecal microbiota from kwashiorkor and healthy co-twins from family 196 into gnotobiotic mice fed Malawian and RUTF diets. (**A**) Discordant weight loss in recipient mice ($n = 10$ mice per group, $^*P < 0.05$, Student's t test). Data points are colored by recipient group: blue, kwashiorkor co-twin fecal microbiota recipients; red, healthy co-twin fecal microbiota recipients. Error bars indicate SEM. (**B**) Average ± SEM (error bars) PC1 coordinate obtained from the weighted UniFrac distances shown in fig. S9, A and B, for fecal microbiota sampled from mice over time. Same color key as in (A). (**C**) Heatmap of phylotypes assigned to species-level taxa whose representation in the fecal microbiota of gnotobiotic mice changed significantly ($P < 0.05$, Student's t test with Bonferroni correction) as a function of donor microbiota and Malawian versus RUTF diets. Asterisks indicate taxa that changed significantly in both healthy and kwashiorkor microbiota transplant recipients. Species level taxa are colored by phylum: red, Firmicutes; blue, Actinobacteria; black, Bacteroidetes; and green, Proteobacteria. Switching from a Malawian diet to RUTF produces a rapid change in the configuration of the transplanted kwashiorkor microbiota. A bloom in *Lactobacilli* occurs early during treatment with RUTF but regresses by the end of this diet period and remains unchanged when animals are returned to the Malawian diet. *Bifidobacterium* spp. also bloom early during administration of RUTF. Unlike the *Lactobacilli*, the increase of *Bifidobacterium* is sustained into the early phases of M2, after which they diminish. Like the members of *Bifidobacterium*, *R. torques* increases its representation during RUTF and then rapidly diminishes when mice returned to a Malawian diet. The increase in *F. prausnitzii* is sustained into and through M2. The responses of the Bacteroidales were opposite to that of the other three groups: Bacteroidales decrease with the administration of RUTF and re-emerge with M2. The response of the *Lactobacilli* observed in the kwashiorkor transplant recipients is not seen in gnotobiotic mice containing the healthy co-twin's microbiota. The pattern of change of the two *Ruminococcus* spp., *B. uniformis*, *P. distasonis*, *B. longum*, and an unclassified *Bifidobacterium* taxon is shared by both recipient groups (healthy and kwashiorkor), although the *Bifidobacterium* response is more diminutive in the healthy microbiota treatment group. *Parabacteroides merdae*, an unclassified taxon from the genus *Faecalibacterium*, as well as a member of the *Coriobacteriaceae*, are specifically elevated in the healthy co-twin's microbiota when mice switch to a RUTF diet. Of these, only *P. merdae* does not persist when animals are returned to the Malawian diet (also see tables S7A and S8A).

treatment group (Fig. 2C and tables S7A, S7B, and S8A). These changes were representative of those that occurred in the human donors; the change in *Bifidobacterium* was unique to the kwashiorkor co-twin (table S9).

Metabolic profiles associated with kwashiorkor. Gas chromatography–mass spectrometry analyses of short-chain fatty acids and 69 other products of carbohydrate, amino acid, nucleotide, and lipid (fatty acid) metabolism in cecal and fecal samples collected during the different diet periods (n = 4 to 5 mice per family-196 microbiota donor) showed that levels of the majority of these metabolites increased when mice were switched to RUTF. In contrast, levels of several di- and monosaccharides (maltose, gentibiose, and tagatose) decreased (fig. S10). There were a number of significant differences between the two groups of mice while they were consuming the different diets (Fig. 3). Although switching to RUTF produced a significant increase in fecal levels of six essential amino acids (valine, leucine, isoleucine, methionine, phenylalanine, and threonine) and three nonessential amino acids (alanine, tyrosine, and serine) in both groups, the response was initially greater in the kwashiorkor group. Four weeks after returning to a Malawian diet, levels of six of these amino acids remained higher in the healthy microbiota recipient group than before consumption of RUTF, but in the kwashiorkor group, these values fell to pre-RUTF–treatment levels (fig. S11, A and B). We observed the same pattern of transient response with urea cycle intermediates in the kwashiorkor group (fig. S11C). RUTF-associated increases in levels of propionate, butyrate, lactate, and succinate were generally greater in mice harboring the healthy co-twin's microbiota (fig. S12A). Similarly, acetate levels were elevated early on during RUTF in the healthy but not the kwashiorkor microbiota (fig. S12A). Increases in these end products of fermentation were accompanied by reductions in the levels of a number of mono- and disaccharides (fig. S12B). The observed differences in metabolic profiles were not attributable to differences in microbial community biomass: There were no statistically significant differences in fecal DNA content between recipients of the healthy and kwashiorkor co-twin microbiota when assayed at the midpoint of RUTF treatment [986.5 ± 108.3 (mean ± SEM) versus 903.2 ± 97.7 ng DNA/mg feces, respectively; P = 0.22, Student's t test] or 4 weeks after cessation of treatment (559.7 ± 62.2 versus 651.6 ± 98.9 ng DNA/mg feces, respectively; P = 0.44). (For characterization of gnotobiotic recipients of family-57 transplants, including taxonomic and metabolic responses to the different diets that they share with family-196 recipients, see supplementary text; fig. S7, C and D; and tables S7C, S7D, S8C, S8D, S9, and S10.)

Microbial-host cometabolism as a function of donor microbiota and host diet. We used standard ^{1}H nuclear magnetic resonance (NMR) spectroscopy to generate urine metabolite profiles (Table 1, fig. S15, and supplementary text) (*26*). A pronounced metabolic shift seen in response to RUTF was not sustained on reintroduction of the Malawian diet; urinary metabolic profiles at the end of the second Malawian diet period (M2) resembled those from the first period (M1), with renewed differentiation between healthy and kwashiorkor microbiota transplant groups. The kwashiorkor microbiota–associated metabolic phenotype was not as distinctive in M2 as it was during M1. When we reanalyzed the data after excluding the RUTF samples, the metabolic differentiation was more apparent between the two Malawian dietary periods (fig. S15, A to C).

Among the notable results, we found that levels of urinary taurine were affected by both donor microbiota and diet. Mice colonized with microbiota from a healthy donor excreted more taurine while consuming both the Malawian diet and RUTF compared with mice with a kwashiorkor microbiota; in both recipient groups, urinary taurine levels were higher when mice consumed a Malawian diet (Table 1). *B. wadsworthia* grows well on bile acids and uses taurine from taurine-conjugated bile acids as a terminal electron acceptor, converting it to ammonia, acetate, and sulfide (*27*). In agreement with this property, fecal levels of *B. wadsworthia* showed an inverse relationship with urinary taurine levels. Levels were higher in the kwashiorkor group; even when the mice were consuming RUTF, recipients of the kwashiorkor microbiota exhibited significantly lower urinary taurine levels and significantly higher fecal levels of *B. wadsworthia* (Table 1 and table S8, A and B). In addition to urinary taurine levels, fecal methionine and cysteine concentrations were significantly lower in mice harboring kwashiorkor compared with those carrying healthy co-twin microbiota when consuming a Malawian diet (Fig. 3). Dietary methionine and cysteine meet most of the human body's needs for sulfur; these amino acids are more abundant in animal and cereal proteins than in vegetable proteins. The Malawian diet is

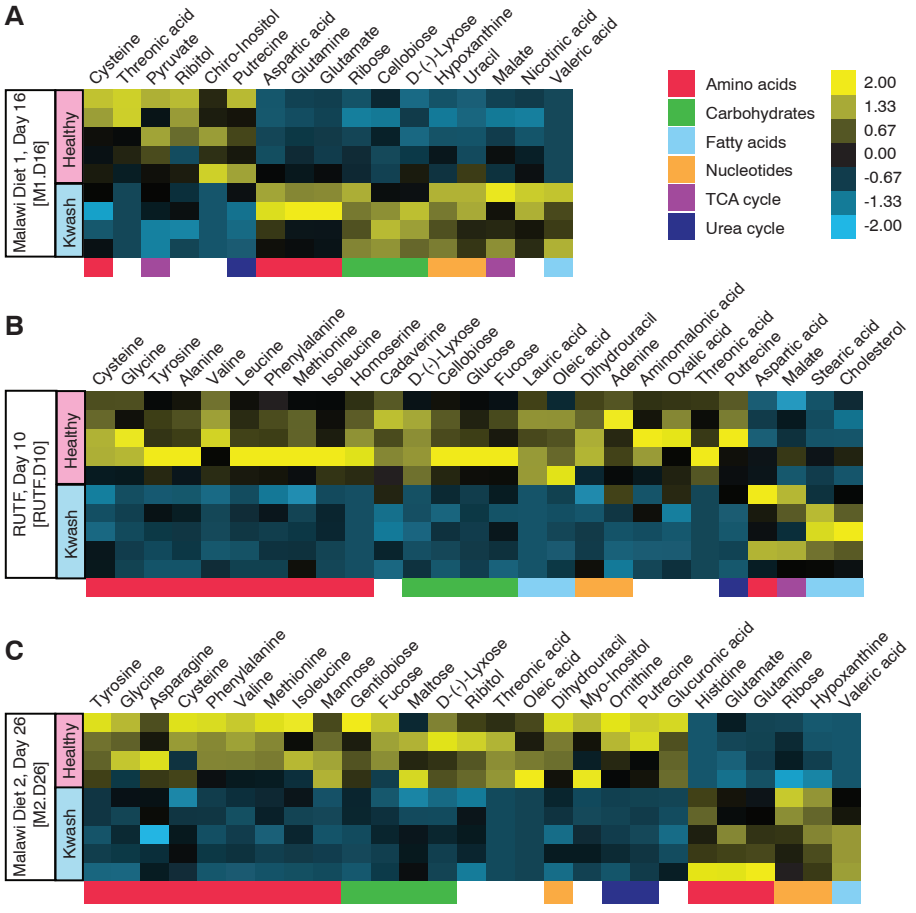

Fig. 3. Metabolites with significant differences in their fecal levels in gnotobiotic mice colonized with microbiota from discordant twin pair 196 as a function of diet. Data are from fecal samples collected 3 days before the end of (**A**) the first period of consumption of the Malawian diet (M1, day 16; abbreviated M1.D16), (**B**) RUTF treatment (RUTF.D10), and (**C**) the second period of Malawian diet consumption (M2. D26). Significant differences are defined as $P < 0.05$, according to Student's t test. Procrustes analysis of data obtained from the transplanted microbiota from discordant co-twins in family 196 (fig. S13) revealed a significant correlation between metabolic and taxonomical profiles on each diet with an overall goodness of fit (M^2 value) of 0.380 ($P < 0.0001$; 1000 Monte Carlo label permutations) for all diets and microbiota.

Table 1. Metabolite analysis of urine samples obtained from mice with transplanted healthy or kwashiorkor co-twin microbiota from family 196 at each diet phase. R^2X represents the variation in ^1H NMR spectral data explained by the O-PLS-DA model, where a value of 1 would indicate that 100% of the variation in the spectral data set is explained by the model. Q^2Y represents the predictive ability of the model and is calculated by leaving a percentage of the data out (15%) while calculating the ability of the model to discriminate between classes in any pairwise comparison (e.g., kwashiorkor versus healthy). Additionally, Q^2Y indicates the level of robustness or significance of the metabolic differences between two classes. The numbers in each column are obtained from median fold normalized O-PLS-DA models and represent the correlation between the NMR data (relative concentration of urinary metabolite) and a given class (e.g., healthy versus kwashiorkor co-twin microbiota or Malawi diet 1 versus RUTF diet). The greater the Q^2Y or predictive value for the O-PLS-DA comparison of two classes, the stronger or more reliable the composite metabolic differences are between two classes (e.g., dietary periods). The closer to 1.0 the correlation value is for any given metabolite, the more weight that metabolite has in discriminating between those two classes. Metabolites are colored according to their over-representation in a treatment group. (**A**) Urinary metabolites with differences in their levels in mice transplanted with the healthy co-twin versus the kwashiorkor co-twin microbiota within a given diet. Color code: blue, higher in kwashiorkor co-twin microbiota recipients; red, higher in healthy co-twin microbiota recipients; white, no significant difference between kwashiorkor and healthy. (**B**) Urinary metabolites with differences in their representation of mice transplanted with healthy or kwashiorkor co-twin microbiota between diets. Color code: red, higher during the M1 diet phase relative to RUTF or relative to M2; orange, higher on RUTF relative to M1 or M2; blue, higher on M2 compared to RUTF or M1; white, no significant differences in the indicated diet comparison.

A

	M1	RUTF	M2
R^2X	0.38	0.49	0.36
Q^2Y	0.62	0.8	0.78
2-oxoadipate	0.8747	0.9069	0.6603
taurine		0.8578	0.6236
lactate			0.4618
creatine	0.9303		
creatinine	0.7692		
methylamine	0.6755	0.8338	0.7646
dimethylamine	0.7732		
trimethylamine	0.8469		
trimethylamine *N*-oxide			
phenylacetylglycine	0.8522	0.8816	
indoxyl sulfate	0.6591	0.8138	
hippurate	0.6301	0.9485	0.9786
allantoin	0.7662		

Higher metabolite concentration in recipients of kwashiorkor co-twin microbiota

Higher metabolite concentration in recipients of healthy co-twin donor microbiota

B

	Recipients of healthy co-twin donor microbiota			Recipients of kwashiorkor co-twin donor microbiota		
	M1 vs RUTF	RUTF vs M2	M1 vs M2	M1 vs RUTF	RUTF vs M2	M1 vs M2
R^2X	0.66	0.58	0.61	0.74	0.52	0.67
Q^2Y	0.57	0.94	0.31	0.87	0.93	0.68
2-oxoglutarate	0.7448	0.8538		0.9062	0.8761	
citrate	0.7065	0.7921		0.827	0.7137	
succinate	0.6794	0.6841		0.8348	0.846	
fumarate	0.7439	0.7553				
acetate				0.7		
2-oxoadipate	0.8382	0.6198				
taurine	0.632	0.7469			0.5998	
lactate	0.5558					0.4733
creatine		0.7432		0.9474	0.759	0.8781
creatinine				0.8297	0.7051	0.6838
methylamine					0.7562	
dimethylamine			0.7469			
trimethylamine	0.7149	0.6639			0.8534	0.878
trimethylamine *N*-oxide					0.799	
phenylacetylglycine		0.8447		0.5716		0.6616
indoxyl sulfate	0.8021	0.8699		0.9593		
hippurate		0.8602				
allantoin		0.8203		0.9133	0.93	0.769
1-methylnicotinamide						0.7554

Higher metabolite concentration during Malawian diet phase 1

Higher metabolite concentration during RUTF

Higher metabolite concentration during Malawian diet phase 2

deficient in total protein and in animal protein. Studies have found a decrease of serum methionine levels and urinary sulfate excretion in patients with kwashiorkor (*28*–*33*). Moreover, cysteine or methionine deficiency in experimental animals can produce weight loss (correctable by sulfate supplementation) (*34*–*36*). Our findings suggest that the combination of a kwashiorkor microbiota and a Malawian diet may contribute to abnormal sulfur metabolism, thereby affecting the pathogenesis and manifestations of this form of SAM.

For mice containing the healthy co-twin's microbiota, urinary excretion of tricarboxylic acid (TCA) cycle intermediates 2-oxoglutarate, citrate, succinate, and fumarate were closely coupled together. These mitochondrial metabolites typically follow similar reabsorption control mechanisms in the renal tubule that are closely linked to tubular pH. In mice containing kwashiorkor microbiota, urinary fumarate excretion was effectively decoupled from the other TCA intermediates (fig. S15, D to G). Differential excretion rates of TCA intermediates can occur where there is selective enzymatic inhibition of the TCA cycle (*37*). The TCA cycle also appears to be disrupted in the kwashiorkor microbiota itself (threefold increase in cecal levels of succinate; $P < 0.05$, unpaired Student's t test), and an increased succinate-to-fumarate ratio (0.58 versus 0.23, $P < 0.05$, unpaired Student's t test while on the Malawian diet) suggests inhibition of succinate dehydrogenase, the enzyme responsible for converting succinate to fumarate. Taken together, these observations suggest that the kwashiorkor microbiota examined in these gnotobiotic mice may generate chemical products that result in a selective inhibition of one or more TCA cycle enzymes, making energy metabolism a bigger challenge for these children when they are exposed to a micro- and macronutrient-deficient, low-calorie diet.

Prospectus. The discordance rate for kwashiorkor is high for both MZ and DZ twins in our study population. Our results illustrate the value of using twins discordant for nutritional phenotypes to characterize the interrelationship between the functional development of the gut microbiome in children and their nutritional status. Linking metagenomic analyses with dietary experiments in gnotobiotic mice that have received gut microbiota transplants from twins discordant for kwashiorkor allowed us to gain insights into pathogenesis by identifying transmissible features associated with healthy versus diseased donors. By replicating a human donor's gut community in multiple recipient mice, we have been able to mimic a clinical intervention and identify community characteristics, including differences in taxonomic composition and in taxonomic and metabolic responses to RUTF. The resulting data provide biomarkers of community metabolism and of microbial-host cometabolism that delineate and discriminate diet and microbiota effects, including biomarkers indicative of the more labile, short-lived nature of the responses of microbiota from kwashiorkor donors to RUTF. The

interrelationships between diet, microbiota, and many facets of host physiology can be explored in detail in these "personalized" gnotobiotic mouse models. These models may be useful for developing new and more effective approaches for treatment and/or prevention. In addition, studies of other forms of malnutrition that take an approach analogous to that described here could also provide insights about the contribution of the gut microbiome to this global health problem.

References and Notes

1. United Nations (UN) Inter-Agency Group for Child Mortality Estimation, *Levels & Trends in Child Mortality Report* (2011); www.childinfo.org/files/Child_Mortality_Report_2011.pdf.
2. WHO Multicentre Growth Reference Study Group, *Acta Paediatr. Suppl.* **450**, 76 (2006).
3. WHO, UN Children's Fund, *WHO Child Growth Standards and the Identification of Severe Acute Malnutrition in Infants and Children* (2009); www.who.int/nutrition/publications/severemalnutrition/9789241598163/en/index.html.
4. C. D. Williams, B. M. Oxon, H. Lond, *Lancet* **226**, 1151 (1935).
5. T. Ahmed, S. Rahman, A. Cravioto, *Indian J. Med. Res.* **130**, 651 (2009).
6. C. Gopalan, in *Calorie Deficiencies and Protein Deficiencies: Kwashiorkor and Marasmus: Evolution and Distinguishing Features*, R. A. McCance, E. M. Widdowson, Eds. (Churchill, London, 1968), pp. 48–58.
7. M. H. Golden, *Lancet* **319**, 1261 (1982).
8. H. Ciliberto *et al.*, *BMJ* **330**, 1109 (2005).
9. C. A. Lin *et al.*, *J. Pediatr. Gastroenterol. Nutr.* **44**, 487 (2007).
10. T. Yatsunenko *et al.*, *Nature* **486**, 222 (2012).
11. R. E. Black *et al.*, *Lancet* **371**, 243 (2008).
12. WHO, World Food Programme, UN System Standing Committee on Nutrition, UN Children's Fund, *Community-Based Management of Severe Acute Malnutrition* (2007); www.who.int/nutrition/topics/statement_commbased_malnutrition/en/index.html.
13. Materials and methods are available as supplementary materials on *Science* Online.
14. L. Lagrone, S. Cole, A. Schondelmeyer, K. Maleta, M. J. Manary, *Ann. Trop. Paediatr.* **30**, 103 (2010).
15. J. Liu *et al.*, *J. Clin. Microbiol.* **50**, 98 (2012).
16. M. Taniuchi *et al.*, *Diagn. Microbiol. Infect. Dis.* **71**, 386 (2011).
17. M. Taniuchi *et al.*, *Am. J. Trop. Med. Hyg.* **84**, 332 (2011).
18. M. Taniuchi *et al.*, *Diagn. Microbiol. Infect. Dis.* **73**, 121 (2012).
19. S. Devkota *et al.*, *Nature* **487**, 104 (2012).
20. N. Crum-Cianflone, *Am. J. Med. Sci.* **337**, 480 (2009).
21. T. Itoh, Y. Fujimoto, Y. Kawai, T. Toba, T. Saito, *Lett. Appl. Microbiol.* **21**, 137 (1995).
22. M. F. Fernández, S. Boris, C. Barbés, *J. Appl. Microbiol.* **94**, 449 (2003).
23. Y. Kato-Mori *et al.*, *J. Med. Food* **13**, 1460 (2010).
24. A. A. Salyers, S. E. West, J. R. Vercellotti, T. D. Wilkins, *Appl. Environ. Microbiol.* **34**, 529 (1977).
25. H. Sokol *et al.*, *Proc. Natl. Acad. Sci. U.S.A.* **105**, 16731 (2008).
26. O. Beckonert *et al.*, *Nat. Protoc.* **2**, 2692 (2007).
27. H. Laue, K. Denger, A. M. Cook, *Appl. Environ. Microbiol.* **63**, 2016 (1997).
28. J. C. Edozien, E. J. Phillips, W. R. F. Collis, *Lancet* **275**, 615 (1960).
29. R. G. Whitehead, R. F. Dean, *Am. J. Clin. Nutr.* **14**, 313 (1964).
30. S. Awwaad, E. A. Eisa, M. El-Essawy, *J. Trop. Med. Hyg.* **65**, 179 (1962).
31. G. Arroyave, D. Wilson, C. DeFunes, M. Béhar, *Am. J. Clin. Nutr.* **11**, 517 (1962).
32. T. R. Ittyerah, S. M. Pereira, M. E. Dumm, *Am. J. Clin. Nutr.* **17**, 11 (1965).
33. T. R. Ittyerah, *Clin. Chim. Acta* **25**, 365 (1969).
34. D. H. Baker, *Prog. Food Nutr. Sci.* **10**, 133 (1986).
35. N. Orentreich, J. R. Matias, A. DeFelice, J. A. Zimmerman, *J. Nutr.* **123**, 269 (1993).
36. M. Mori, S. Manabe, K. Uenishi, S. Sakamoto, *Tokushima J. Exp. Med.* **40**, 35 (1993).
37. J. K. Nicholson, J. A. Timbrell, P. J. Sadler, *Mol. Pharmacol.* **27**, 644 (1985).

Acknowledgments: We thank S. Wagoner, J. Manchester, and M. Meier for superb technical assistance; J. Manchester, S. Deng, and J. Hoisington-López for assistance with DNA sequencing; M. Karlsson, D. O'Donnell, and S. Wagoner for help with gnotobiotic mouse husbandry; W. Van Treuren for writing several scripts, B. Mickelson (Teklad Diets) and H. Sandige for assistance with the design of the mouse diets; and members of the Gordon lab for valuable suggestions during the course of this work. This work was supported by grants from the Bill & Melinda Gates Foundation, and the NIH (DK30292, DK078669, T32-HD049338). M.I.S was the recipient of a postdoctoral fellowship from the St. Louis Children's Discovery Institute (MD112009-201). J.V.L was the recipient of an Imperial College Junior Research Fellowship. Illumina V4-16S rRNA and 454 shotgun pyrosequencing data sets have been deposited with the European Bioinformatics Institute. Specifically, human: V4-16S rRNA data sets (ERP001928) and shotgun sequencing data sets (ERP001911). Mouse: gnotobiotic recipients of discordant twin pair 196: V4-16S rRNA data sets (ERP001861); gnotobiotic recipients of discordant twin pair 196: shotgun sequencing data sets (ERP001819); gnotobiotic recipients of discordant twin pair 57: V4-16S rRNA data sets (ERP001871); gnotobiotic recipients of discordant twin pair 57: shotgun sequencing data sets (ERP001909). Twin pairs were recruited through health centers located in Makhwira, Mitondo, M'biza, Chamba, and Mayaka. Recruitment of participants for the present study, clinical protocols, sample collection procedures, and informed consent documents were all reviewed and approved by the College of Medicine Research Ethics Committee of the University of Malawi and by the Human Research Protection Office of Washington University in St. Louis. All experiments involving mice were performed using protocols approved by the Washington University Animal Studies Committee. Author contributions: M.I.S., T.Y., and J.I.G designed the experiments; M.J.M. designed and implemented the clinical monitoring and sampling for the trial; R.M. and I.T. participated in patient recruitment, sample collection, sample preservation, and clinical evaluations; M.I.S. performed experiments involving gnotobiotic mice, whereas T.Y. characterized microbiota obtained from twins; M.I.S., T.Y., J.C., A.L.K., S.S.R., P.C., J.C.M., J.L., E. Houpt, J.V.L., E. Holmes, and J.N. generated data; M.I.S., T.Y., E. Holmes, J.N., D.K, L.K.U, R.K., and J.I.G. analyzed the results; and M.I.S., T.Y., and J.I.G. wrote the paper.

Supplementary Materials

www.sciencemag.org/cgi/content/full/339/6119/548/DC1
Materials and Methods
Supplementary Text
Figs. S1 to S15
Tables S1 to S10
References (*38*–*54*)

17 August 2012; accepted 10 December 2012
10.1126/science.1229000

REPORTS

A Clock Directly Linking Time to a Particle's Mass

Shau-Yu Lan,[1] Pei-Chen Kuan,[1] Brian Estey,[1] Damon English,[1] Justin M. Brown,[1] Michael A. Hohensee,[1] Holger Müller[1,2]*

Historically, time measurements have been based on oscillation frequencies in systems of particles, from the motion of celestial bodies to atomic transitions. Relativity and quantum mechanics show that even a single particle of mass *m* determines a Compton frequency $\omega_0 = mc^2/\hbar$, where *c* is the speed of light and $\hbar$ is Planck's constant *h* divided by 2π. A clock referenced to ω_0 would enable high-precision mass measurements and a fundamental definition of the second. We demonstrate such a clock using an optical frequency comb to self-reference a Ramsey-Bordé atom interferometer and synchronize an oscillator at a subharmonic of ω_0. This directly demonstrates the connection between time and mass. It allows measurement of microscopic masses with 4×10^{-9} accuracy in the proposed revision to SI units. Together with the Avogadro project, it yields calibrated kilograms.

A particle with mass-energy $E = mc^2$ is represented by a wave oscillating at the Compton frequency $\omega_0 = mc^2/\hbar$ in the particle's rest frame, where *c* is the speed of light and $\hbar$ is Planck's constant *h* divided by 2π (*1*). This is the basis of de Broglie's theory of matter waves (*2*) and underpins modern quantum mechanics and field theory: The time evolution of states is given by wave equations whose plane-wave solutions are proportional to

$$e^{-i\phi} = \exp(-ip_\mu x^\mu/\hbar) = \exp(-i\omega_0\tau) \qquad (1)$$

where $p_\mu = (-m\gamma, m\gamma\boldsymbol{v})$ and x^μ are the momentum and position four-vector, $\tau = t/\gamma$ is the proper time, γ is the Lorentz factor, and $\boldsymbol{v}$ and *t* are the laboratory-frame velocity and time. Much has been theorized about the physical reality of quantum states as "oscillators" (*3*–*7*), but surprisingly few experiments have been proposed to address this topic (*8*). Here, we directly address a consequence of Eq. 1 that has deep physical and perhaps even cosmological implications: Because the oscillations of a wave packet accumulate phase $\omega_0\tau$ just like a clock following the same

[1]Department of Physics, 366 Le Conte Hall MS7300, University of California, Berkeley, CA 94720, USA. [2]Lawrence Berkeley National Laboratory, One Cyclotron Road, Berkeley, CA 94720, USA.

*To whom correspondence should be addressed. E-mail: hm@berkeley.edu